2232 Bull. Chem. Soc. Jpn. Vol. 80, No. 11, 2232–2242 (2007)

The Alkylation of Biphenyl over One-Dimensional Twelve-Membered Ring Zeolites. The Influence of Zeolite Structure and Alkylating Agent on the Selectivity for 4,4′-Dialkylbiphenyl

Yoshihiro Sugi,*[1] Hiroyoshi Maekawa,[1] Akira Ito,[1] Chikako Ozawa,[1]
Tomoko Shibata,[1] Akihiro Niimi,[1] Chihara Asaoka,[1] Kenichi Komura,[1]
Yoshihiro Kubota,[1,†] Jae-Youl Lee,[2] Jong-Ho Kim,[2] and Gon Seo[2]

[1]Department of Materials Science and Technology, Faculty of Engineering, Gifu University, Gifu 501-1193

[2]School of Applied Chemical Engineering and The Research Institute for Catalysis, Chonnam National University, Gwangju 500-757, Korea

Received April 2, 2007; E-mail: ysugi@gifu-u.ac.jp

Alkylation, i.e., isopropylation, *s*-butylation, and *t*-butylation, of biphenyl (BP) was examined over one-dimensional twelve-membered (12-MR) zeolites: Mordenite (MOR) and SSZ-24 (AFI) with straight channels, and SSZ-55 (ATS) and SSZ-42 (IFR) with corrugated channels. Types of zeolites and alkylating agents highly influenced the selectivities for dialkylbiphenyl (DABP) isomers. Shape-selective formation of 4,4′-diisopropylbiphenyl (4,4′-DIPB) was observed over MOR and AFI; however, ATS and IFR gave 4,4′-DIPB only in low selectivities at 250 °C: 87% over MOR, 60% over AFI, 20% over ATS, and 30% over IFR. The selectivities for 4,4′-di-*s*-butylbiphenyl (4,4′-DSBB) in the *s*-butylation were higher than those for 4,4′-DIPB: 95% over MOR, 85% over AFI, 75% over ATS, and 50% over IFR. The *t*-butylation afforded selectively 4,4′-di-*t*-butylbiphenyl (4,4′-DTBB) over the zeolites: 96–97% over MOR and AFI, 90% over ATS, and 80% over IFR. These results in the alkylation indicate the exclusion of 4,4′-DABP from other bulky DABP isomers by steric restriction in zeolite channels is an important key for the high shape-selectivity. Even zeolites with large channels, such as ATS and IFR, can have shape-selective nature if the bulky moieties, such as *s*-butyl and *t*-butyl groups, are large enough to differentiate the transition state of the least bulky 4,4′-DABP from those of the other isomers inside their channels. The selectivity for 4,4′-DABP decreased at high temperatures in some alkylations: isopropylation over MOR, and *s*-butylation and *t*-butylation over MOR, AFI, and ATS. The decreases are due to the isomerization of 4,4′-DABP at external acid sites, because the channels are not large enough for the isomerization of 4,4′-DABP to bulkier 3,4′-DABP. However, the isopropylation over AFI was accompanied by the isomerization of 4,4′-DIPB at external and internal acid sites, because the channels are large enough for the isomerization of 4,4′-DIPB.

Shape-selective catalyses by zeolites occur by differentiating reactants, products, and/or reaction intermediates according to their shapes and sizes in the sterically restricted environments of the zeolites.[1–6] Only molecules that have dimensions less than a critical size can enter zeolite pore and react at the internal catalytic sites, and the bulky molecules, which cannot accommodate in the channels, are excluded from the channels, resulting in the preferential formation of the least bulky isomers. Furthermore, only molecules that can diffuse through the channels will appear in the products.

Isopropylation of biphenyl (BP) is a typical acid-catalyzed reaction for demonstrating shape-selective nature of molecular sieves.[4–12] Selective formation of the least bulky 4,4′-diisopropylbiphenyl (4,4′-DIPB) should be facilitated over ordered microporous materials if the catalytic sites are appropriately restricted by steric hindrance in their channels. In previous papers, we have described that 4,4′-DIPB is selectively produced from BP over dealuminated H-mordenite, which has 12-membered (12-MR) pore-entrance with straight channels.[4–10] Shape-selective isopropylation of BP have also been described over one-dimensional zeolites, ZSM-12,[13] CIT-5,[13–15] SSZ-24,[13,15,16] SAPO-5,[17] MAPO-5 (M: Mg, Ca, Sr, Ba, and Zn),[18] and SSZ-31.[13,19] We have proposed that shape-selective isopropylation over these zeolites occurred by effective exclusion of the transition states of bulkier DIPB isomers by the steric restriction inside the channels, resulting in preferential formation of 4,4′-DIPB.[4–10,13–19] On the other hand, Takeuchi et al. have reported that the isopropylation of BP over Y-zeolite afforded principally thermodynamically unstable DIPB isomers with 2-isopropyl group at low temperatures and thermodynamically stable isomers, 3,4′-, 3,3′-, and 4,4′-DIPB at high temperatures.[20] Similar results were also obtained in the isopropylation over Beta and CIT-1 zeolites.[21] These results indicate that the isopropylation occurs under kinetic control at lower temperatures and under thermodynamic control at high temperatures because the channels of these zeolites are too large for the selective formation of 4,4′-DIPB.[4–7]

Alkylating agent is another important key for shape-selective catalysis. Bulky alkylating agent increases the steric restrictions on the transition states of bulky isomers inside the

---

[†] Present address: Department of Materials Science and Engineering, Graduate School of Engineering, Yokohama National University, Yokohama 240-8501

Published on the web November 13, 2007; doi:10.1246/bcsj.80.2232

Table 1. Properties of Zeolites

Zeolite	FTC	Pore entrance /nm^2	Structure of channel	Cage (MR)	SiO_2/Al_2O_3	Surface area /m^2 g^{-1}	External surface area /m^2 g^{-1} $^{a)}$	Pore volume /mL g^{-1}	NH_3-TPD peak temp. /°C	Acid amount /mmol g^{-1}
Mordenite	MOR	0.67 × 0.72	Straight with 8-MR side-pocket	—	128	460	35	0.16	389	0.20
SSZ-24	AFI	0.72 × 0.72	Straight	—	202	414	5.4	0.16	274	0.11
SSZ-55	ATS	0.65 × 0.75	Corrugated	20	160	478	18	0.19	299	0.12
SSZ-42	IFR	0.62 × 0.72	Corrugated	24	280	518	11	0.20	255	0.08

a) Calculated by *t*-plot of N_2 adsorption.

channels and enhance the difference in bulkiness among the isomers, resulting in preferential formation of the least bulky isomers. There have been only a few papers involving the influence of the alkylating agent on the alkylation of BP.[15,20,22–25] Horniakova et al. have described that the use of 2-methyl-2-propanol as alkylating agent afforded the high selectivity for 4,4′-di-*t*-butylbiphenyl (4,4′-DTBB) in the *t*-butylation over MOR, Y, and Beta zeolites.[22–24] We also found that the shape-selectivities in *s*-butylation and *t*-butylation occurred over one-diemensional 14-MR zeolites: CIT-5, UTD-1, and SSZ-53,[15] and over three-dimensional 12-MR zeolites: Y, β, and CIT-1.[21]

It is interesting to elucidate how the zeolite structures, particularly, dimensionality, pore-entrance, and channel structure, are related to the shape-selective catalysis. In recent decades, new types of 12-membered ring (12-MR) aluminosilicates with different pore and channel structures have been synthesized by many workers.[14,16,26–39] SSZ-24 zeolite[27–30] has straight channels with pore-entrance of 0.72 nm × 0.72 nm.[26] SSZ-55[31–34] and SSZ-42[35–39] zeolites have corrugated channels: 20-MR cavities with pore entrance of 0.65 nm × 0.75 nm and 24-MR cavities with pore entrance of 0.62 nm × 0.72 nm, respectively.[26]

In this paper, we describe the alkylation, i.e., isopropylation, *s*-butylation, and *t*-butylation, of BP over one-dimensional 12-MR zeolites, and discuss the influence of the selectivities for dialkylbiphenyl (DABP) isomers on the structure of zeolite: straight channels for Mordenite and SSZ-24 zeolites and corrugated channels for SSZ-55 and SSZ-42 zeolites. We also focus on the influence of bulkiness of alkylating agents on the alkylation over these zeolites. The discussion in the paper was based on the selectivity for DABP isomers to understand the relationships between zeolite structure and alkylating agent in shape-selective catalysis. The abbreviations of zeolites are expressed by FTC from IZA Structure Commission: MOR for Mordenite, AFI for SSZ-24, ATS for SSZ-55, and IFR for SSZ-42,[26] or as stated otherwise.

Experimental

Zeolites. AFI, IFR, and ATS were synthesized according to the literatures.[30–32,35] MOR was obtained commercially from Tosoh Corp., Tokyo, ($SiO_2/Al_2O_3 = 128$; TSZ-690HOA). All zeolites were used as H-form and calcined at 550–650 °C before the reaction.

The zeolites were characterized by FE-SEM, XRD, ICP, N_2 and *o*-xylene adsorption, NH_3-TPD, and ^{11}B, ^{27}Al, and ^{29}Si MAS NMR. Properties of the zeolites related to the catalysis are summarized in Table 1.

The Alkylation of BP. The alkylation of BP was carried out in a 100-mL SUS-316 autoclave. Typical reaction conditions of the isopropylation were: BP 7.71 g (50 mmol), the catalyst 0.25 g, temperature 150–300 °C, and period 4 h under 0.8 MPa of propene pressure 0.8 MPa (0.4 MPa for 1-butene in the *s*-butylation and for 2-methylpropene in the *t*-butylation). An autoclave containing BP and the catalyst was purged with nitrogen and heated to reaction temperature, and the reaction started by agitation after introduction of propene into the autoclave. The pressure was maintained constant throughout the reaction. After cooling the autoclave to ambient temperature and careful release of excess propene, the catalyst was separated from organic products by filtration. The organic products were subjected to the analyses by using a Gas Chromatograph GC-14A or GC-18A (Shimadzu Corp., Kyoto) equipped with an Ultra-1 capillary column (25 m × 0.2 mm; Agilent Technologies Co., Ltd., MA, USA). The products were also identified by using a Shimadzu Gas Chromatograph-Mass Spectrometer GC-MS 5000.

Dialkylbiphenyl in the alkylation is generally expressed as DABP: DIPB, DSBB, and DTBB for isopropylation, *s*-butylation, and *t*-butylation, respectively.

The yields of each product in the alkylation of BP were calculated on the basis of the amount of starting BP, and the selectivities for each DABP isomer were determined based on total amounts of DABP isomers, respectively.

$$\text{Selectivity for a DABP isomer (\%)} = \frac{\text{Each DABP isomer (mol)}}{\text{DABP isomers (mol)}} \times 100. \quad (1)$$

The catalytic activities based on the yield of alkylates are summarized in Figs. S1–S6 of the Supporting Information.

Analysis of the encapsulated products in the catalyst used for the reaction was carried out as follows. The catalyst, separated from organic products by filtration, was washed well with 200 mL of acetone, and dried at 110 °C for 12 h. A 50-mg sample of the resulting catalyst was carefully dissolved in 3 mL of aqueous hydrofluoric acid (47%) at room temperature. This solution was neutralized with solid potassium carbonate, and the organic layer was extracted three times with 20 mL of dichloromethane. After removal of the solvent in vacuo, the residue was again dissolved in toluene (5 mL), and subjected to GC analysis according to the same procedure as the analysis for bulk products.

The Characterization of Catalysts. The crystal structure of zeolites was determined by powder X-ray diffraction using a Shimadzu XRD-6000 diffractometer with Cu Kα radiation ($\lambda = 1.5418$ Å). Elemental analysis of zeolites was performed by using inductive coupled plasma atomic emission spectroscopy on

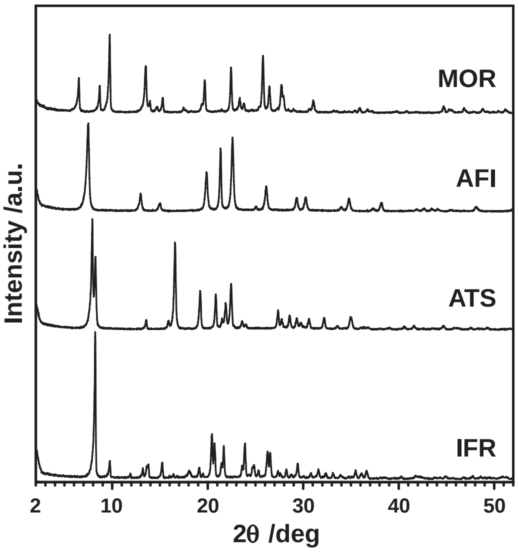

Fig. 1. XRD patterns of 12-MR zeolites used as catalysts.

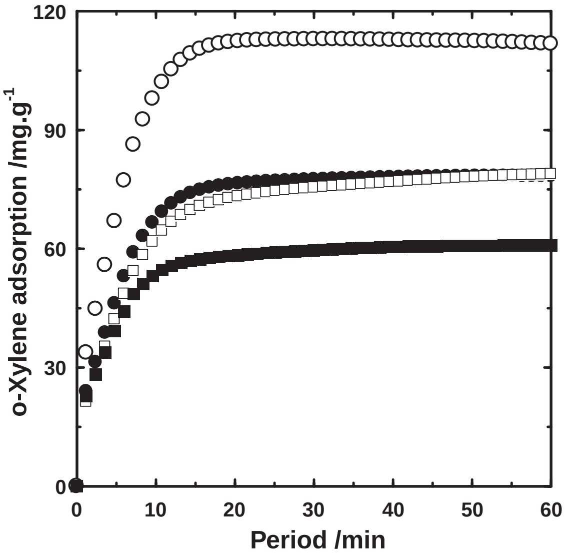

Fig. 3. o-Xylene adsorption on zeolites: ■: MOR; □: AFI; ●: ATS; ○: IFR.

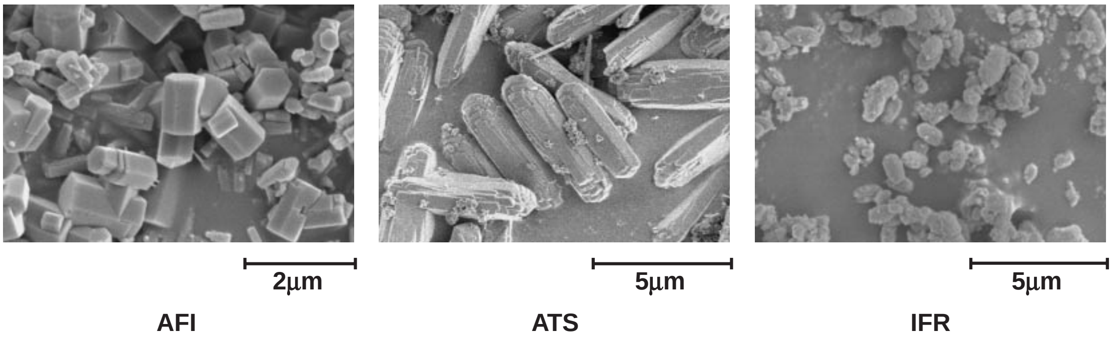

Fig. 2. SEM images of 12-MR zeolites (as-synthesized) used for the catalysis.

a JICP-PS-1000 UV spectrometer (Teledyne Leeman Labs, Inc., NH, USA). Crystal size and morphology of zeolites were determined on an S-4300 FE-SEM microscope (Hitachi Corp., Tokyo). N_2 adsorption measurements were carried out on a Belsorp 28SA apparatus (Bel Japan, Inc., Osaka). The adsorption of o-xylene was performed by gravimetric method with its vapor (0.48 kPa) using a highly sensitive quartz microbalance at 120 °C after the evacuation at 550 °C. Ammonia temperature programmed desorption (NH_3-TPD) was measured by using a TPD-66 apparatus (Bel Japan): the catalyst sample was evacuated at 400 °C for 1 h, and ammonia was adsorbed at 100 °C followed by further evacuation for 1 h. Then, the sample was heated from room temperature to 710 °C at the rate of 10 °C min^{-1} in a helium flow. ^{11}B, ^{27}Al, and ^{29}Si NMR spectra were recorded at room temperature under magic angle spinning (MAS) by using 7.0 mm diameter zirconia rotors spinning at 4 kHz on an Inova 400 spectrometer (Varian Corp., MA, USA).

Results and Discussion

Properties of Zeolites. Typical physicochemical properties of the zeolites, MOR, AFI, ATS, and IFR, used for the catalysis, are shown in Table 1. These properties agree with those of the zeolites in the literature.[14,16,26–39]

Figure 1 shows the XRD patterns of MOR, AFI, ATS, and IFR. Figure 2 shows typical SEM images of the as-synthesized samples. XRD patterns and SEM images of these zeolites agree with those in the literature.[14,28–30,37–39]

Substitution of B^{3+} in [B]-SSZ-42 and [B]-SSZ-55 with Al^{3+} was carried out by using 1 M $Al(NO_3)_3$ aqueous solution (1 M = 1 mol dm^{-3}) at 80 °C according to the literature.[15] XRD patterns after repeating the substitution three times were almost the same as original calcined samples. The structure of zeolites did not collapse during calcination, acid treatment, and substitution of B^{3+} with Al^{3+}.

N_2 adsorption on MOR, AFI, ATS, and IFR exhibited a typical type-I isotherm (Figure not shown). Their specific surface area and pore volume were 410–520 m^2 g^{-1} and 0.16–0.20 mL g^{-1}, respectively. These results indicate that MOR, AFI, ATS, and IFR have typical microporous structures. External surface areas calculated from t-plot of N_2 adsorption were 35, 5.4, 14, and 11 m^2 g^{-1} for MOR, AFI, ATS, and IFR.

Figure 3 shows the adsorption of o-xylene on MOR, AFI, ATS, and IFR. The adsorption was saturated in short period on all zeolites. The initial rates of the adsorption were in the order: IFR (28.1 m^2 g^{-1} min^{-1}) > ATS (19.9 m^2 g^{-1} min^{-1}) ≥ MOR (19.0 m^2 g^{-1} min^{-1}) ≥ AFI (17.7 m^2 g^{-1} min^{-1}). In addition, the amounts of the adsorption were significantly

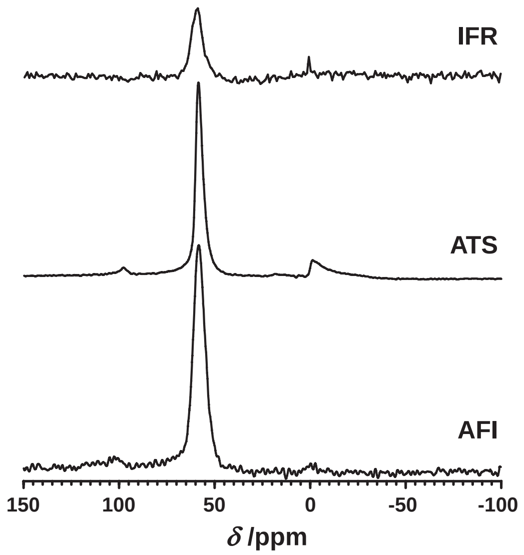

Fig. 4. ^{27}Al MAS NMR spectra of 12-MR zeolites.

influenced by the types of zeolites in the order: IFR $\gg$ ATS $\geq$ AFI $>$ MOR. It means that their channels are large enough for the diffusion of *o*-xylene in them. These results of *o*-xylene adsorption are ascribed to the space in the channels of zeolites: ATS and IFR have corrugated channels with 20-MR and 24-MR cages and with pore-entrance of 0.65 nm × 0.75 nm and 0.62 nm × 0.72 nm, respectively; however, MOR and AFI have straight channels with pore-entrance of 0.67 nm × 0.72 nm and 0.72 nm × 0.72 nm, respectively.[26] These differences may reflect their catalytic properties in the alkylation of BP.

^{27}Al MAS NMR spectra of AFI, ATS, and IFR are shown in Fig. 4. Peaks assigned to tetrahedral Al^{3+} species, which are incorporated to zeolite framework, were observed at around 50 ppm in all zeolites. Small octahedral Al^{3+} species, which are not incorporated in the framework, appeared at around 0 ppm after substitution of B^{3+} in the frameworks of [B]-SSZ-42 and [B]-SSZ-55 with Al^{3+}. However, AFI synthesized from [Al]-BEA as a precursor only had small peaks of octahedral Al^{3+} species. Tetrahedral and octahedral Al^{3+} species also appeared in the spectra of AFI prepared from [B]-SSZ-24.[16] Substitution of B^{3+} with Al^{3+} was also confirmed in the ^{11}B and ^{29}Si MAS NMR spectra.

NH_3-TPD profiles of MOR, AFI, ATS, and IFR are shown in Fig. 5. They had *l*- and *h*-peaks in the range of around 150–250 and 250–450 °C, respectively. *l*-Peaks are due to physical adsorption, and *h*-peaks correspond to Brønsted acidity by Al^{3+} species incorporated in the zeolite framework judging from the observation with ^{27}Al MAS NMR. Acid amounts, calculated from area of deconvoluted *h*-peak, reflect the SiO_2/Al_2O_3 ratios (see Table 1). The peak temperature of *h*-peak was the highest for MOR and decreased in the order: MOR (389 °C) $\gg$ ATS (294 °C) $>$ AFI (274 °C) $>$ IFR (255 °C), which corresponds to the order of acid strength (see Table 1). AFI, ATS, and IFR have weaker acidities than MOR; particularly, IFR has the lowest acidity among four zeolites. However, their acidities are enough for the acid catalysis, particularly, alkylation of polynuclear aromatic hydrocarbons, such as BP.

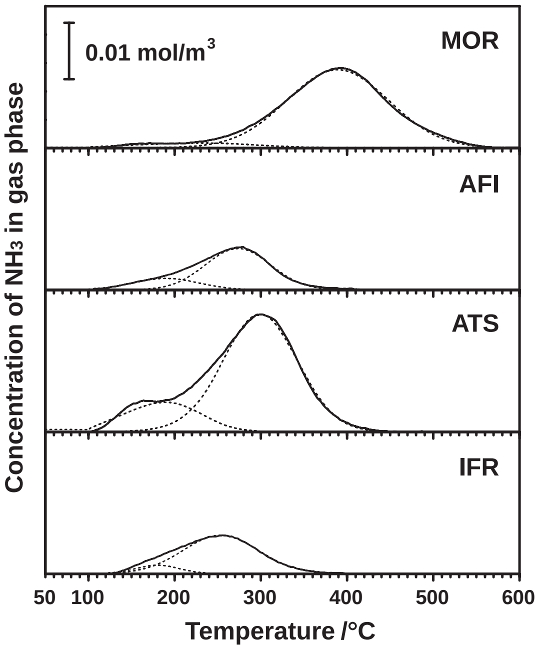

Fig. 5. NH_3-TPD profiles of zeolites. Dotted lines: *l*- and *h*-Peaks by the deconvolution.

The Isopropylation. Figure 6 shows the influence of reaction temperature on the isopropylation of BP over MOR and AFI. The selectivities for 4,4′-DIPB were 90% over MOR and 50–65% over AFI at low to moderate temperatures up to 275 °C. Similar features of the selectivity for 4,4′-DIPB were observed over AFI prepared by the substitution of B^{3+} in [B]-SSZ-24 with Al^{3+}.[16] These results at moderate temperatures mean that 4,4′-DIPB is formed inside the channels through shape-selective catalysis by "restricted transition state selectivity mechanisms."[1] Bulky DIPB isomers are preferentially excluded from their channels by steric restriction, resulting in the selective formation of 4,4′-DIPB as discussed previously.[4–10] However, the selectivity for 4,4′-DIPB over AFI was lower than that over MOR at moderate temperatures, because AFI has larger channels than MOR.

The selectivity in bulk products decreased to 30% at 300 °C accompanying the increase in the formation of 3,4′- and 3,3′-DIPB as shown in Fig. 6. However, the selectivity for 4,4′-DIPB in encapsulated products over MOR was around 90% in the range of 150–300 °C. These results show that the decrease in the selectivity for 4,4′-DIPB over MOR is due to the isomerization of 4,4′-DIPB at the external acid sites as discussed in the previous paper.[4–10,40] On the other hand, the selectivity for 4,4′-DIPB in bulk products over AFI was 65–70% up to 275 °C and decreased to 30% at 300 °C. The selectivity for 4,4′-DIPB in encapsulated products also decreased gradually from 70% at 250 °C to 50% at 300 °C. These results indicate that 4,4′-DIPB is isomerized at the acid sites, partly inside the channels in addition to at the external surface. These differences in the isomerization of 4,4′-DIPB between MOR and AFI are due to the steric restriction in zeolite channels. AFI can allow the accommodation of the transition states of the bulkier DIPB isomers inside the channels, because its channels are larger than those of MOR. However, there is another possibility that the decrease in steric restriction by AFI channels

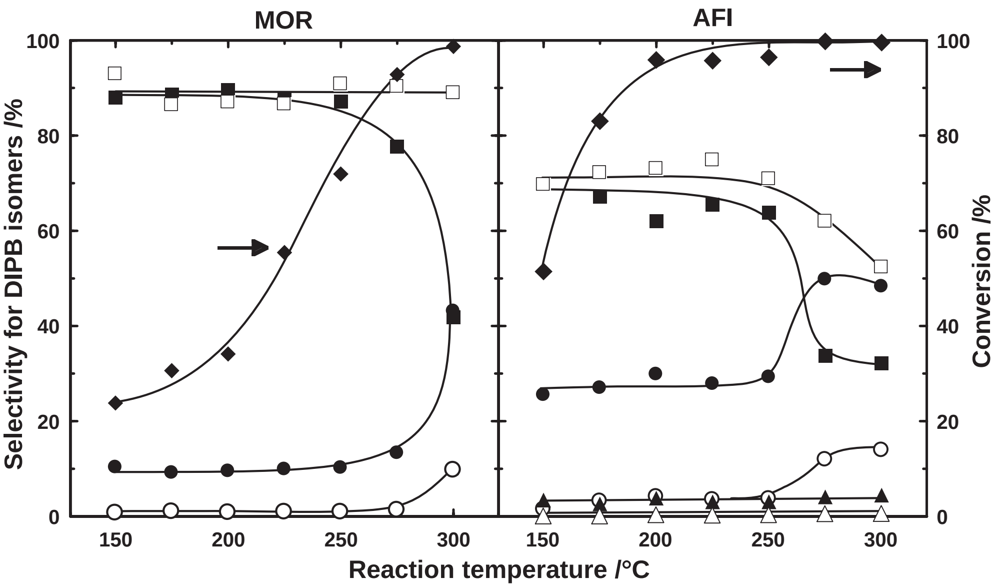

Fig. 6. The influence of reaction temperature on the isopropylation of BP over MOR and AFI. Reaction conditions: for MOR: BP, 30.84 g (200 mmol); catalyst, 1.0 g and for AFI: BP, 7.71 g (50 mmol); catalyst, 0.25 g; temperature, 150–300 °C; propene pressure, 0.8 MPa; period, 4 h. Legends: Bulk products. ■: 4,4′-DIPB; ●: 3,4′-DIPB; ○: 3,3′-DIPB; ▲: 2,*x*′-DIPB; △: 3,5-DIPB; ◆: conversion. Encapsulated products. □: 4,4′-DIPB.

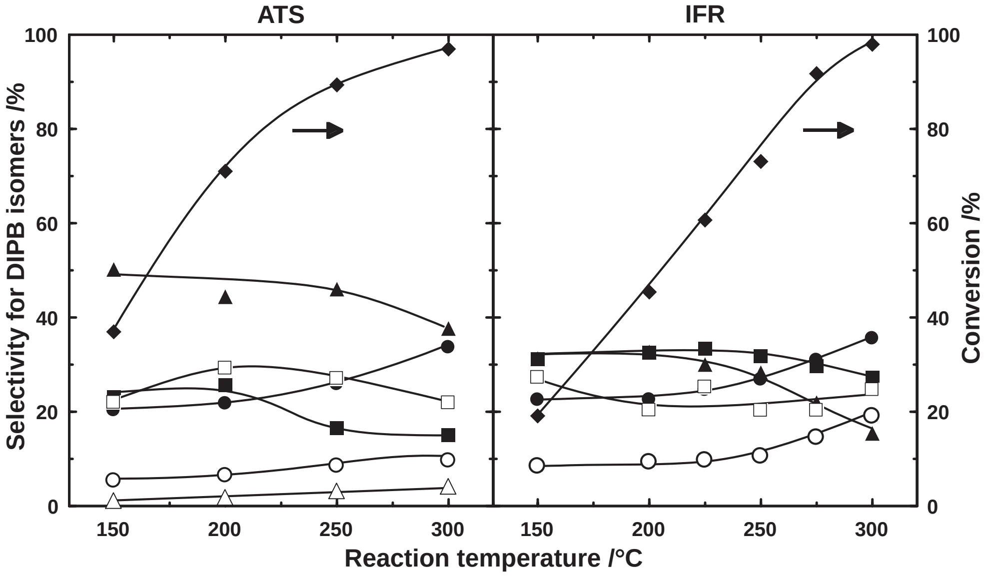

Fig. 7. The influence of reaction temperature on the isopropylation of BP over ATS and IFR zeolites. Reaction conditions: for ATS: BP, 7.71 g (50 mmol); catalyst, 0.25 g and for IFR: 3.86 g (25 mmol); catalyst, 0.125 g; temperature, 150–300 °C; propene pressure, 0.8 MPa; period, 4 h. Legends: see Fig. 6.

causes the decease in the selectivity for 4,4′-DIPB at high temperatures. Isomerization of 4,4′-DIPB inside the channels was also observed for MAPO-5 (M: Mg and Zn) with AFI topology[18] and for CIT-5 with CFI topology.[13–15]

Figure 7 shows the influence of reaction temperature on the isopropylation of BP over ATS and IFR. The selectivities for 4,4′-DIPB over ATS and IFR were much lower than those over MOR and AFI. The selectivity for 4,4′-DIPB was only 23% at 150 °C to 15% at 300 °C over ATS and 35% at 150 °C to 28% at 300 °C over IFR. The principal products over ATS and IFR were bulky DIPB isomers, 2,*x*′-DIPB (2,2′-, 2,3′- and 2,4′-DIPB) and 3,4′-DIPB, and the selectivity for 2,*x*′-DIPB decreased at higher temperatures, accompanied by an increase in the selectivity for 3,4′-DIPB. These high selectivities for 2,*x*′-DIPB and 3,4′-DIPB resemble the isopropylation of BP over FAU, BEA, and CON.[20,21] The low selectivities for 4,4′-DIPB over these zeolites are due to loose steric restriction on the transition states of bulky DIPB isomers in corrugated channels: the formation of bulky 2,*x*′-DIPB is allowed inside the channels, resulting in the low selectivity for 4,4′-DIPB. Over these zeolites, the increase in the reaction temperature caused the decrease in the selectivity for 2,*x*′-DIPB and the

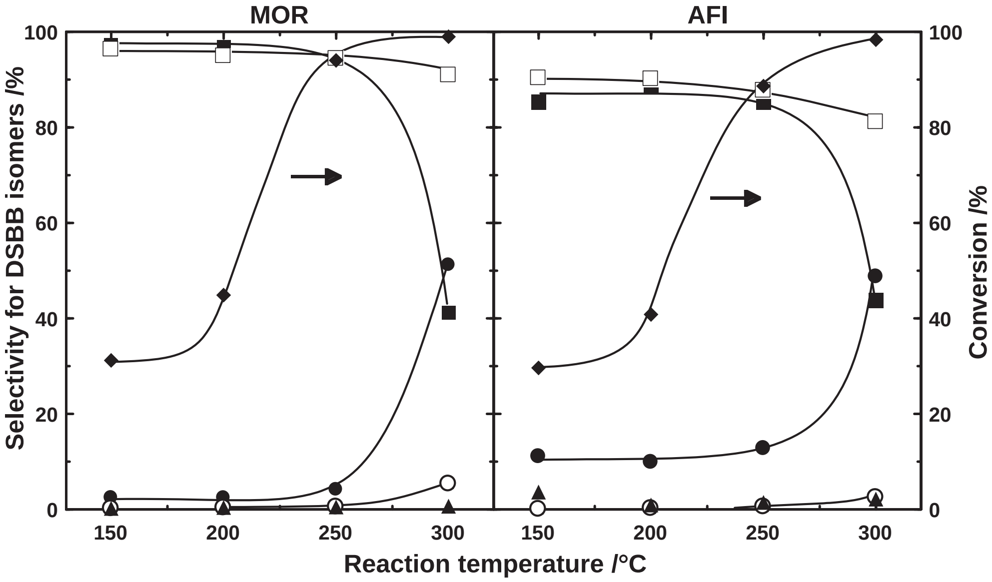

Fig. 8. The influences of reaction temperature on the *s*-butylation of BP over MOR and AFI. Reaction conditions: for MOR: BP, 7.71 g (50 mmol); catalyst, 0.25 g and for AFI: BP, 3.86 g (25 mmol). catalyst, 0.125 g; temperature, 150–300 °C; 1-butene pressure, 0.5 MPa; period, 4 h. Legends: Bulk products. ■: 4,4′-DSBB; ●: 3,4′-DSBB; ○: 3,3′-DSBB; ▲: 2,*x*′-DSBB; ◆: conversion. Encapsulated products. □: 4,4′-DSBB.

increase in the selectivity for 3,4′- and 3,3′-DIPB. These results suggest that the formation of 2,*x*′-DIPB over ATS and IFR is kinetically controlled at lower temperatures, because of the predominant nucleophilic attack of alkylating agent at the 2-position of BP, which has a high electron density; however, the decrease in the selectivity for 2,*x*′-DIPB was accompanied by an increase in the selectivity for thermodynamically stable 3,4′- and 3,3′-DIPB with an increase in the temperature.

The selectivities for 4,4′-DIPB in encapsulated products in the isopropylation over ATS and IFR are also shown in Fig. 7. They were 20–30% for ATS and IFR: these values were almost constant at all temperatures. These results strongly indicate that low selectivities for 4,4′-DIPB over ATS and IFR are due to kinetic and thermodynamic control in the catalysis, and not to the isomerization of 4,4′-DIPB formed shape-selectively inside the channels.

The selectivities for 4,4′-DIPB over SSZ-24 zeolites were on the same level as those over SAPO-5 and MAPO-5 (M: Mg, Ca, Sr, and Zn) in the isopropylation of BP.[17,18] SSZ-55 and MAPO-36 (M: Mg and Zn) also gave similar level of the selectivities for 4,4′-DIPB.[41,42] These results show that the selectivities by the zeolites with AFI and ATS topologies do not depend on the type of metals, but on the type of framework.

The *s*-Butylation. Figure 8 summarizes the influence of reaction temperature on the *s*-butylation of BP over MOR and AFI. The selectivities for 4,4′-di-*s*-butylbiphenyl (4,4′-DSBB) among DSBB isomers were enhanced significantly compared to those in the isopropylation. The selectivities for 4,4′-DSBB were higher than 95% over MOR and 90% over AFI at low and moderate temperatures below 250 °C. The selectivities for 4,4′-DSBB in the *s*-butylation were higher than those for 4,4′-DIPB in the isopropylation. Although the effective molecular diameter of DSBB isomers is almost the same as that of DIPB isomers, the replacement of isopropyl groups with the *s*-butyl groups in 3,4′- and 4,4′-DABP causes the differences in bulkiness of both DABP isomers at the interaction of the transition states with the channels. These synergetic effects enhance the shape-selectivities for 4,4′-DSBB over MOR and AFI by replacement of isopropyl group with *s*-butyl group.

Figure 9 shows the influence of reaction temperature on the *s*-butylation of BP over ATS and IFR. The selectivities for 4,4′-DSBB were 70% over ATS and 50% over IFR at 250 °C, and they were much higher than those for 4,4′-DIPB in the isopropylation. These results indicate that shape-selective natures appeared in the *s*-butylation even over corrugated ATS and IFR channels, although they are less effective than those over MOR and AFI. *s*-Butyl moieties of DSSB isomers may exclude more effectively the transition states leading to bulky isomers, such as 3,4′-DSBB, by steric restriction in ATS and IFR channels. The selectivities for 4,4′-DSBB over ATS were higher than those over IFR. ATS makes easier to exclude the bulkier isomers at their transition states than IFR, because ATS have smaller reaction space than IFR. A decrease in the selectivity for 2,*x*′-DSBB occurred over ATS and IFR at high temperatures accompanying the formation of 3,4′-DSBB: this is due to the participation of kinetic control to yield predominantly 2,*x*′-DIPB at lower temperatures and of thermodynamic control to yield 3,4′-DIPB at higher temperatures.

The selectivities for 4,4′-DSBB in bulk products decreased at high temperatures in the range of 250–300 °C in the *s*-butylation in Fig. 8 for MOR and AFI and in Fig. 9 for ATS and IFR. However, the selectivities for 4,4′-DSBB in encapsulated products remained high over these zeolites. These results mean that these decreases are due to the isomerization of 4,4′-DSBB at external acid sites, which cannot occur inside the channels as discussed in the isopropylation.[4–10] The channels of these zeolites are too small for the isomerization of 4,4′-DSBB.

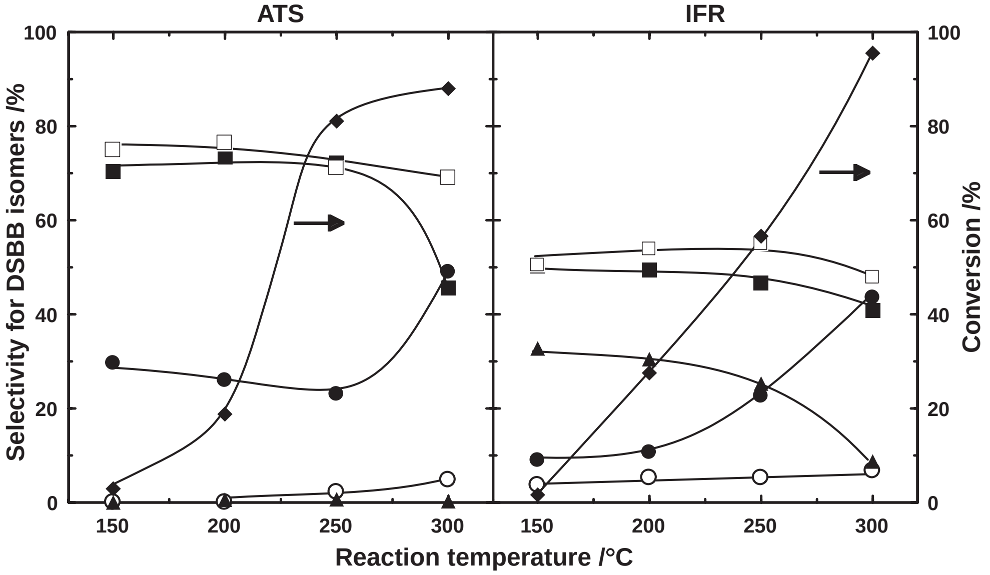

Fig. 9. The influences of reaction temperature on the *s*-butylation of BP over ATS and IFR. Reaction conditions. 3.86 g (25 mmol); catalyst, 0.125 g; temperature, 150–300 °C; 1-butene pressure, 0.5 MPa; period, 4 h. Legends: see Fig. 8.

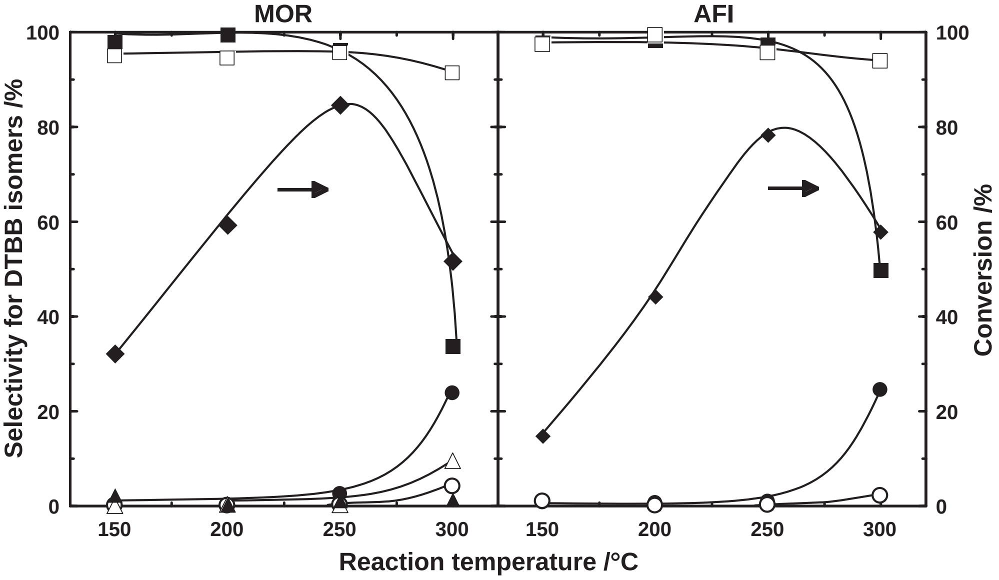

Fig. 10. The influences of reaction temperature on the *t*-butylation of BP over MOR and AFI. Reaction conditions: for MOR: BP, 7.71 g (50 mmol); catalyst, 0.25 g and for AFI: BP, 3.86 g (25 mmol); catalyst, 0.125 g; temperature: 150–300 °C; 2-methylpropene pressure, 0.5 MPa; period: 4 h. Legends. Bulk products: ■: 4,4′-DTBB; ●: 3,4′-DTBB; ○: 3,3′-DTBB; ▲: 2,*x*′-DTBB; ◆: conversion. Encapsulated products: □: 4,4′-DTBB.

On the other hand, there were no significant changes in the selectivity for 4,4′-DSBB in bulk and encapsulated products over IFR. This may be due to low acidities of IFR judging from NH_3-TPD.

The *t*-Butylation. The influence of reaction temperature on the *t*-butylation of BP is shown in Fig. 10 for MOR and AFI and in Fig. 11 for ATS and IFR. Shape-selective formation of 4,4′-DTBB was observed over these zeolites at low and moderate temperatures, and the selectivities for 4,4′-DTBB at 250 °C were higher than those for 4,4′-DIPB and 4,4′-DSBB in isopropylation and *s*-butylation: 95% over MOR and AFI, 90% over ATS, and 80% over IFR. These results shows the channels of these zeolites can differentiate 4,4′-DTBB from other bulky isomers at the transition states. However, the less selective formation of 4,4′-DTBB over ATS and IFR is due to loose steric restriction on the transition states of the bulky isomers inside their channels. Particularly, the large IFR channels allow the formation of bulkier 3,4′-DTBB.

The selectivities for 4,4′-DTBB in encapsulated DTBB isomers in the *t*-butylation over these zeolites remained high in the range of 150–250 °C as shown in Figs. 10 and 11: 95–98% over MOR and AFI, and 85–93% over ATS, and 75–83% over IFR. However, the selectivities for 4,4′-DTBB in bulk products were significantly lowered at 300 °C over

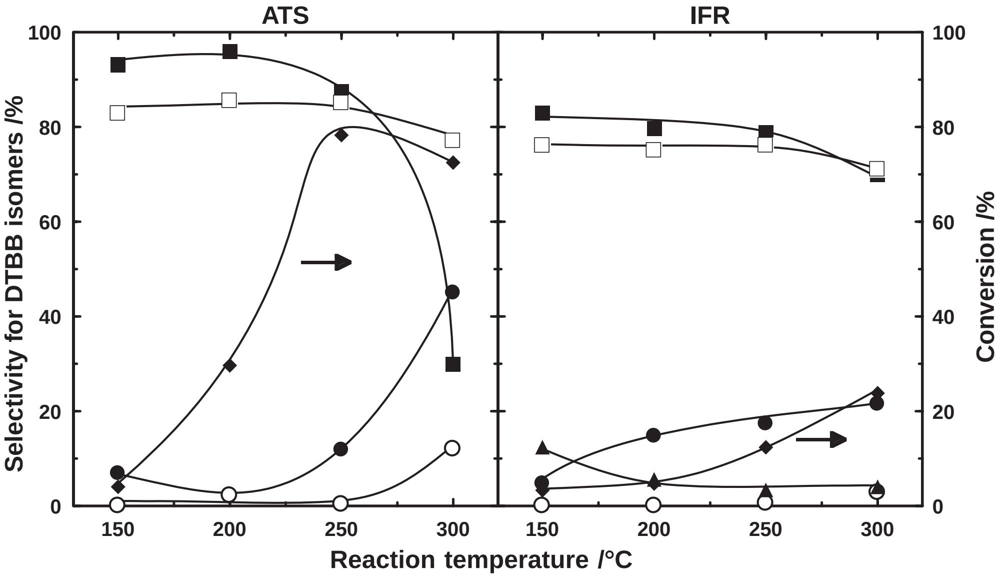

Fig. 11. The influences of reaction temperature on the *s*-butylation of BP over ATS and IFR. Reaction conditions: BP, 3.86 g (25 mmol); catalyst, 0.125 g.; temperature, 150–300 °C; 2-methylpropene pressure, 0.5 MPa; period, 4 h. Legends: see Fig. 10.

MOR, AFI, and ATS: 30% over MOR and ATS, and 50% over AFI. The differences in the selectivities for 4,4′-DTBB between bulk and encapsulated products over MOR, AFI, and ATS indicate that the isomerization of 4,4′-DTBB occurs at the external acid sites because the channels of these zeolites are too small for the isomerization of 4,4′-DTBB. On the other hand, no significant change in the selectivities for 4,4′-DTBB occurred over IFR: the external acid sites of IFR are less active in the catalysis compared to those of the other zeolites, because of the low acidity discussed in the *s*-butylation.

Decreases in the conversion of BP were observed in the *t*-butylation over MOR and AFI, accompanied by decreases in the yield of DTBB isomers (see Fig. S5 in the Supporting Information). These decreases are due to the de-alkylation of DTBB isomers at the higher temperatures.

The Influence of Zeolite Structure and Alkylating Agent. MOR, AFI, ATS, and IFR are one-dimensional zeolites with 12-MR pore-entrances, although they have different types of channels. MOR and AFI have straight channels with pore-entrance of 0.67 nm × 0.72 nm and 0.73 nm × 0.73 nm, respectively.[26] ATS and IFR have corrugated channels: 20-MR cavities with pore entrance of 0.65 nm × 0.75 nm and 24-MR cavities with pore entrance of 0.62 nm × 0.72 nm, respectively. (see also in Fig. S7 in the Supporting Information).[26] The features indicate that the reaction space inside channels is in the order: MOR $<$ AFI $\ll$ ATS $<$ IFR, and consequently, that the steric restriction in the channels decreases in the order: MOR $>$ AFI $\gg$ ATS $>$ IFR. These differences reflect the exclusion of bulky DABP isomers from the channels.

Figure 12 shows the selectivities for DABP isomers in bulk products and for 4,4′-dialkylbiphenyl (4,4′-DABP) in encapsulated products in the alkylation of BP over MOR, AFI, ATS, and IFR at 250 °C. They were typical selectivities in relation to the zeolite structure, because further isomerization of 4,4′-DABP are almost negligible over these zeolites at 250 °C. The products from the alkylation of BP are classified into three categories: 4,4′-DABP for the least bulky isomer by the shape-selective catalysis, 3,*x*′-DABP (3,4′- and 3,3′-) for the thermodynamically stable and bulky isomers formed principally under thermodynamic control, and 2,*x*′-DABP (2,2′-, 2,3′-, and 2,4′-) for the bulky and thermodynamically unstable isomers formed principally under kinetic control. The selectivities for 4,4′-, 3,*x*′-, and 2,*x*′-DABP highly depended on the type of zeolites and alkylating agents. Particularly, the selectivities for 4,4′-DABP decreased with an increase in the reaction spaces in the zeolites and increased with an increase in bulkiness of the alkylating agents. The selectivities for 3,*x*′- and 2,*x*′-DABP were also influenced by reaction temperatures in addition to type of zeolites and alkylating agents as discussed in the previous sections. The selectivities for 4,4′-DABP in encapsulated products at 250 °C were similar to those in bulk products, as shown in Fig. 12.

Shape-selective isopropylation of BP, which means the preferential formation of the least bulky 4,4′-DIPB by the exclusion of bulky DIPB isomers due to the steric restriction of the transition states, occurred only over MOR and AFI with straight channels. The lower selectivity for 4,4′-DIPB of AFI compared to that of MOR is due to the loose restriction of AFI channels compared to that of MOR. On the other hand, ATS and IFR with corrugated channels gave 4,4′-DIPB only with a low selectivity, accompanying bulkier isomers, 2,*x*′- and 3,*x*′-DIPB. The large spaces in the channels of ATS and IFR compared to those of MOR and AFI can allow the formation of bulky isomers in their channels. These high selectivities for 2,*x*′-DIPB and 3,*x*′-DIPB resemble the isopropylation over FAU, BEA, and CON.[20,21] Isopropylation under sterically less restricted conditions in zeolite channels is controlled kinetically at low temperatures to yield 2,*x*′-DIPB isomers, because of preferential nucleophilic attack of alkylating agent at 2-position with high electron density. However, the thermodynamic factors contribute to the catalysis at high temperatures, resulting in the enhancement of stable isomers, 3,*x*′-DIPB, particularly, 3,4′-DIPB.

The *s*-butylation gave the high selectivities for 4,4′-DSBB

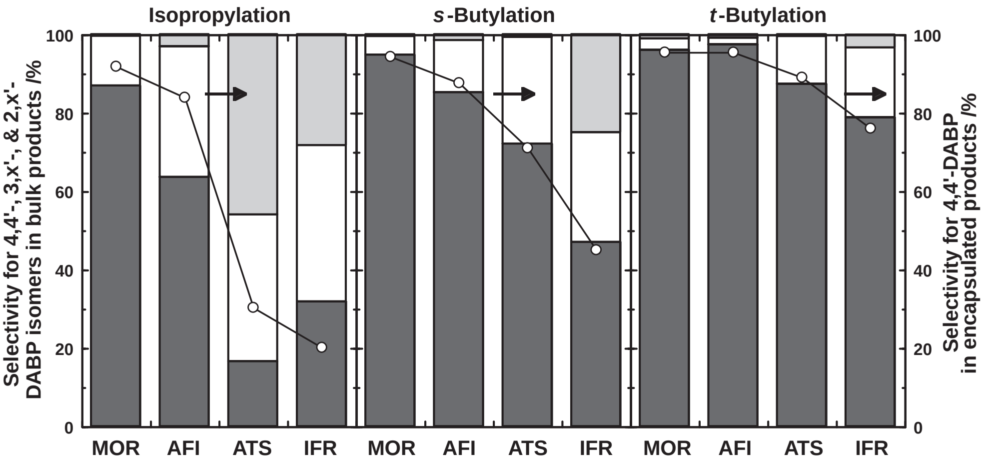

Fig. 12. The selectivity for DABP isomers in the alkylation of BP over the zeolites. Reaction conditions: temperature: 250 °C. Other conditions: see Figs. 6–11. Legends ■: 4,4′-DABP; □: 3,*x*′-DABP (3,4′-, 3,3′-, and 3,5-); ▨: 2,*x*′- DABP (2,2′-, 2,3′-, and 2,4′-); ○: 4,4′-DABP in encapsulated products.

over MOR and AFI at 250 °C: 95% over MOR and 85% over AFI. The selectivities for 4,4′-DSBB were higher than those for 4,4′-DIPB in the isopropylation. They were also enhanced in the *s*-butylation over ATS and IFR: 75% over ATS and 50% over IFR. Although ATS and IFR channels are corrugated, they effectively exclude the bulky isomers in the *s*-butylation, resulting in the selective formation of 4,4′-DSBB. The differences in the selectivities for 4,4′-DSBB are due to the steric restriction of bulky isomers among the zeolites as discussed above. The lower selectivities for 4,4′-DSBB over IFR compared to those over ATS are due to the difference of corrugated channels: 20-MR cages for ATS and 24-MR cages for IFR.[26] The *s*-butylation over ATS and IFR was still controlled kinetically at low temperatures and thermodynamically at higher temperatures. The selectivities for 4,4′-DSBB over ATS and IFR were higher than those over DON with straight 14-MR channels and SFH with corrugated 14-MR channels.[15]

Shape-selective formation of 4,4′-DTBB was observed in the *t*-butylation over all zeolites. The selectivities for 4,4′-DTBB were over 90% over MOR and AFI at 250 °C. As well, ATS and IFR afforded high selectivities for 4,4′-DTBB: 85% over ATS and 80% over IFR. These results mean that the steric restriction of transition states in the channels decreased in the order: MOR ≈ AFI > ATS > IFR, as discussed on the *s*-butylation.

The selectivities for DABP isomers over a zeolite were influenced by the bulkiness of alkylation agents. Highly shape-selective formation of 4,4′-DABP was observed over MOR and AFI in all alkylations. The alkylation over ATS and IFR with corrugated channels was influenced by the types of alkylating agent: the selectivities for 4,4′-DIPB in the isopropylation were 20% over ATS and 30% over IFR at 250 °C, and higher selectivities for 4,4′-DSBB were obtained: 70% over ATS and 50% over IFR. Moreover, the selective formation of 4,4′-DTBB occurred in the *t*-butylation over these zeolites. The bulkiness of alkylating agent enhances the steric interaction of the transition states of DABP isomers with channels. Moreover, the replacement of isopropyl groups with the bulky groups in 3,4′- and 4,4′-DABP causes the differences in bulkiness of both DABP isomers and in the interaction of their transition states with the channels. These synergetic effects enhance the shape-selectivities with increasing the bulkiness of alkylating agents. The channels of ATS and IFR are too large for the selective formation of 4,4′-DIPB in the isopropylation; however, shape-selective natures appeared in *s*-butylation and *t*-butylation over these zeolites. Kinetic control at low temperatures and thermodynamic control at high temperatures contribute principally to the isopropylation, yielding 2,*x*′- and 3,*x*′-DIPB as principal products, respectively. However, the exclusion of the bulky DSBB isomers occurred even inside large ATS and IFR channels in *s*-butylation by using 1-butene, resulting in the increasing the selectivities for 4,4′-DSBB. Further, 4,4′-DTBB were effectively differentiated from bulky DTBB isomers by the channels of these zeolites in the *t*-butylation. The similar influence of alkylating agents on the selectivities for 4,4′-DABP were observed for one-dimensional 14-MR zeolites,[15] and three-dimensional 12-MR zeolites,[21] which have large reaction space in their channels. These results indicate that the shape-selective catalysis occurs through the differentiation of the least bulky isomer from the other isomers in the transition states by steric restriction inside the channels. "Product selectivity mechanism,"[1] in which the least bulky isomers predominantly diffuse out from the mixtures inside the channels, does not occur in these alkylation, because the selective formation of 4,4′-DABP was accompanied by their high selectivities in the encapsulated products.

We have found the shape-selective formation of 4,4′-DIPB in the isopropylation of BP over several one-dimensional 12-MR zeolites with straight channels: ZSM-12,[13] and SSZ-31[19] zeolites as well as MOR and SSZ-24 zeolites. Highly selective formation of 4,4′-DABP has also been observed in the *s*-butylation and the *t*-butylation over SSZ-31[19] as well as over SSZ-24. Particularly, 4,4′-DSBB and 4,4′-DTBB were selectively obtained over SSZ-24 and SSZ-31 zeolites, which have the largest channels among 12-MR zeolites.

The selectivities for 4,4′-DIPB over SSZ-24 were in the same level as those over SAPO-5 and MAPO-5 (M: Mg, Ca, Sr, and Zn) in isopropylation, *s*-butylation, and *t*-butylation of BP.[17,18] Similar results were obtained in the isopropylation over SSZ-55 and MAPO-36 (Mg: Mg and Zn).[41,42] These results show that the selectivities over the zeolites with AFI and ATS topologies do not depend on the type of metals, but on the type of their framework.

Among one-dimensional 14-MR zeolites, CFI yields 4,4′-DIPB shape-selectively in the isopropylation of BP.[13–15] However, the predominant DIPB isomers are 2,*x*′-DIPB with 2-isopropyl group over DON and SFH, and the selectivities for 4,4′-DIPB are 10–15% in both bulk and encapsulated products.[15] The selectivities for 4,4′-DSBB and 4,4′-DTBB were enhanced by using bulky alkylating agent, 1-butene and 2-methylpropene, respectively.[15] Particularly, 4,4′-DTBB was obtained selectively in the *t*-butylation over all zeolites. These differences are due to reaction spaces in the channels by the types of zeolites and to alkylating agents as discussed for 12-MR zeolites in this study.

The selectivity for 4,4′-DABP in bulk products decreased with an increase in the temperatures in some alkylations: isopropylation over MOR, and *s*-butylation and *t*-butylation over MOR, AFI, and ATS. However, the selectivities for 4,4′-DABP in encapsulated products remained high in the alkylation even at the high temperatures as 300 °C. These results suggest that the decreases in the selectivity for 4,4′-DABP are caused by the isomerization of 4,4′-DABP to 3,4′-DABP at the external acid sites, because the channels are too small for the isomerization of 4,4′-DABP as discussed for the isopropylation of BP over MOR.[4–10] On the other hand, the selectivities for 4,4′-DIPB both in bulk and encapsulated products in the isopropylation over AFI decreased with an increase in temperature: this is due to the channels being large enough for the isomerization of 4,4′-DIPB.

Conclusion

Alkylation, i.e., isopropylation, *s*-butylation, and *t*-butylation, of biphenyl (BP) was examined over one-dimensional 12-MR zeolites, Mordenite (MOR), SSZ-24 (AFI), SSZ-55 (ATS), and SSZ-42 (IFR). The selectivities for 4,4′-dialkylbiphenyl (4,4′-DABP) varied with the types of zeolite and alkylating agent. Shape-selective formation of 4,4′-diisopropylbiphenyl (4,4′-DIPB) was observed over MOR and AFI; however, ATS and IFR afforded only low selectivities for 4,4′-DIPB. Increases in the selectivity for 4,4′-di-*s*-butylbiphenyl (4,4′-DSBB) were observed in the *s*-butylation: 95% over MOR, 85% over AFI, 75% over ATS, and 50% over IFR. Further, shape-selective formation of 4,4′-di-*t*-butylbiphenyl (4,4′-DTBB) was oberved in the *t*-butylation over all zeolites. These results indicate that alkylation occurs inside the channels and that the selectivities for DABP isomers reflect the differences in the steric restriction at the transition states inside the channels. The differences in reaction spaces appeared in types of zeolites: straight channels for MOR and AFI, and corrugated channels for ATS and IFR, although they have 12-MR pore-entrance. The former two zeolites have severe steric restriction inside their channels compared to the latter two zeolites. The alkylating agents also invoke the differences in bulkiness of products isomers and in steric restriction inside the channels. From these synergetic effects on the alkylation, the selectivity for 4,4′-DABP over a particular zeolite was governed by the exclusion of bulky isomers at the transition states due to the steric restriction inside their channels. Even zeolites with large channels, such as ATS and IFR, can have shape-selective nature if the bulky moieties, such as *s*-butyl and *t*-butyl groups, are large enough to differentiate the transition state of the least bulky DABP from other isomers inside their channels.

The selectivities for 4,4′-DABP decreased at high temperatures in some alkylations. These decreases are due to the isomerization of 4,4′-DABP, because the channels are not large enough for the isomerization of 4,4′-DABP to bulkier 3,4′-DABP.

A part of this work was financially supported by a Grant-in-Aid for Scientific Research (B) No. 16310056, the Japan Society for the Promotion of Science (JSPS) and by Research Project under the Japan-Korea Basic Scientific Cooperation Program, JSPS and Korea Science and Engineering Foundation (KOSEF; Grant No. F01-2004-000-10510-0).

Supporting Information

Figures S1–S6: The influence of yields of alkylates on the alkylation of BP over MOR, AFI, ATS, and IFR. Figure S7: Models for channels of zeolites. This material is available free of charge on the web at http://www.csj.jp/journals/bcsj.

References

1 S. M. Csicsery, *Zeolites* **1984**, *4*, 202.

2 P. B. Venuto, *Microporous Mater.* **1994**, *2*, 297.

3 N. Y. Chen, W. E. Garwood, F. G. Dwyer, *Shape-Selective Catalysis in Industrial Applications*, 2nd ed., Marcel Dekker, New York, **1996**.

4 Y. Sugi, Y. Kubota, in *Catalysis*, ed. by J. J. Spivey, Specialist Periodical Report, Royal Soc. Chem., **1997**, Vol. 13, pp. 55–84.

5 Y. Sugi, *Korean J. Chem. Eng.* **2000**, *17*, 1.

6 Y. Sugi, Y. Kubota, T. Hanaoka, T. Matsuzaki, *Catal. Surv. Jpn.* **2001**, *5*, 43.

7 Y. Sugi, K. Komura, J.-H. Kim, *J. Korean Ind. Eng. Chem.* **2006**, *17*, 235.

8 T. Matsuzaki, Y. Sugi, T. Hanaoka, K. Takeuchi, H. Arakawa, T. Tokoro, G. Takeuchi, *Chem. Express* **1989**, *4*, 413.

9 Y. Sugi, T. Matsuzaki, T. Hanaoka, Y. Kubota, J.-H. Kim, X. Tu, M. Matsumoto, *Catal. Lett.* **1994**, *27*, 315.

10 Y. Sugi, S. Tawada, T. Sugimura, Y. Kubota, T. Hanaoka, T. Matsuzaki, K. Nakajima, K. Kunimori, *Appl. Catal., A* **1999**, *189*, 251.

11 G. S. Lee, J. J. Maj, S. C. Rocke, J. M. Garces, *Catal. Lett.* **1989**, *2*, 243.

12 D. Vergani, R. Prins, H. W. Kouwenhoven, *Appl. Catal., A* **1997**, *163*, 71.

13 Y. Sugi, Y. Kubota, A. Ito, H. Maekawa, R. K. Ahedi, S. Tawada, S. Watanabe, I. Toyama, C. Asaoka, H. Lee, J.-H. Kim, G. Seo, *Stud. Surf. Sci. Catal.* **2004**, *154*, 2228.

14 H. Maekawa, C. Naitoh, K. Nakagawa, A. Iida, K. Komura, Y. Kubota, Y. Sugi, J.-H. Kim, G. Seo, *J. Mol. Catal. A: Chem.* **2007**, *274*, 24.

15 Y. Sugi, H. Maekawa, S. A. R. Mulla, A. Ito, C. Naitoh, K. Nakagawa, K. Komura, Y. Kubota, J.-H. Kim, G. Seo, *Bull. Chem. Soc. Jpn.* **2007**, *80*, 1418.

16 A. Ito, H. Maekawa, H. Kawagoe, K. Komura, Y. Kubota, Y. Sugi, *Bull. Chem. Soc. Jpn.* **2007**, *80*, 215.

17 M. Bandyopadhyay, R. Bandyopadhyay, S. Tawada, Y.

Kubota, Y. Sugi, *Appl. Catal., A* **2002**, *225*, 51.

18 H. Maekawa, S. K. Saha, S. A. R. Mulla, S. B. Waghmode, K. Komura, Y. Kubota, Y. Sugi, *J. Mol. Catal. A: Chem.* **2007**, *263*, 238.

19 R. K. Ahedi, S. Tawada, Y. Kubota, Y. Sugi, J. H. Kim, *J. Mol. Catal. A: Chem.* **2003**, *197*, 133.

20 G. Takeuchi, H. Okazaki, T. Kito, Y. Sugi, T. Matsuzaki, *Sekiyu Gakkaishi* **1991**, *34*, 242.

21 Y. Sugi, H. Maekawa, Y. Hasegawa, A. Ito, R. Asai, D. Yamamoto, K. Komura, Y. Kubota, J.-H. Kim, G. Seo, *Catal. Today*, in press.

22 J. Horniakova, D. Mravec, S. Fabokova, M. Hronec, P. Moreau, *Appl. Catal., A* **2000**, *203*, 47.

23 J. Horniakova, D. Mravec, P. Moreau, *Catal. Lett.* **2001**, *70*, 163.

24 J. Horniakova, D. Mravec, M. Kralik, J. Lesko, P. Graffin, P. Moreau, *Appl. Catal., A* **2001**, *215*, 235.

25 R. Anand, S. S. Khaire, R. Maheswari, K. U. Gore, *J. Mol. Catal. A: Chem.* **2004**, *218*, 241.

26 IZA Structure Commission. http://www.iza-online.org/.

27 S. I. Zones, U.S. Patent 4,665,110, **1987**.

28 S. I. Zones, Y. Nakagawa, *Microporous Mater.* **1994**, *2*, 557.

29 R. F. Lobo, M. E. Davis, *Microporous Mater.* **1994**, *3*, 61.

30 Y. Kubota, H. Maekawa, S. Miyata, T. Tatsumi, Y. Sugi, *Microporous Mesoporous Mater.* **2007**, *101*, 115.

31 C.-Y. Chen, S. I. Zones, U.S. Patent 6,468,501, **2002**.

32 S. A. Elomari, T. V. Harris, U.S. Patent, 6,475,463, **2002**.

33 S. A. Elomari, S. I. Zones, *Stud. Surf. Sci. Catal.* **2001**, *135*, 479.

34 M. G. Wu, M. W. Deem, S. A. Elomari, R. C. Medrud, S. I. Zones, T. Maesen, C. Kibby, C.-Y. Chen, I. Y. Chan, *J. Phys. Chem. B* **2002**, *106*, 264.

35 S. I. Stacy, U.S. Patent, 5,653,956, **1997**.

36 P. A. Barrett, M. A. Camblor, A. Corma, R. H. Jones, L. A. Villaescusa, *Chem. Mater.* **1997**, *9*, 1713.

37 C. Y. Chen, L. W. Finger, R. C. Medrud, P. A. Crozier, I. Y. Chan, T. V. Harris, S. I. Zones, *Chem. Commun.* **1997**, 1775.

38 C. Y. Chen, L. W. Finger, R. C. Medrud, C. L. Kibby, P. A. Crozier, I. Y. Chan, V. Thomas, L. W. Beck, S. I. Zones, *Chem. Eur. J.* **1998**, *4*, 1312.

39 C. Y. Chen, S. I. Zones, L. T. Yuen, T. V. Harris, S. A. Elomari, Proceedings of the International Zeolite Conference, 12th, **1999**, Vol. III, p. 1945.

40 The equilibrium composition of DIPB isomers at 300 °C: 3,4′- (33%), 3,3′- (37%), 4,4′- (9%), 3,5-DIPB (17%), and others (4%).[20]

41 S. K. Saha, S. B. Waghmode, H. Maekawa, R. Kawase, K. Komura, Y. Kubota, Y. Sugi, *Microporous Mesoporous Mater.* **2005**, *81*, 277.

42 S. K. Saha, H. Maekawa, S. B. Waghmode, S. A. R. Mulla, K. Komura, Y. Kubota, Y. Sugi, S.-J. Cho, *Mater. Trans.* **2005**, *46*, 2659.